24th INTERNATIONAL CONGRESS ON SOUND AND VIBRATION
23–27 July 2017, London

ICSV24
23-27JULY 2017
LONDON CALLING

APPLICATION OF AN ALL-PASS FILTER CASCADE TO ACTIVE VIBRATION CONTROL OF CANTILEVER BEAMS

Jiří Tůma, Pavel Šuránek, Jaroslav Los, Miroslav Mahdal

VSB – Technical University of Ostrava, Faculty of Mechanical Engineering, Ostrava, Czech Republic
email: jiri.tuma@vsb.cz, pavel.suranek@vsb.cz, Jaroslav.los@vsb.cz, Miroslav.mahdal@vsb.cz

The problem of active vibration control of weakly damped mechanical structures is potentially unstable modes of vibrations due to the positive feedback for some vibration modes. The paper will discuss the change of positive feedback on the negative one using all-pass discrete-time filters which are arranged in a cascade. The piezoelectric actuator as a source of force is used to damp vibration. It is well known that this actuator type has hysteresis.
Keywords: active vibration control; all-pass filter; piezo-actuator

1. Introduction

The problem of the active vibration control of weakly damped mechanical structures consists in potentially unstable modes of vibrations. If the gain feedback is increased, then some of the poles of the transfer function in the complex plane recede the stability boundary which is the imaginary axis, while the other poles approach it, even the boundary is crossed for a large feedback gain and the system becomes unstable. In this case, the feedback becomes positive for these vibration modes. The paper will discuss the change of positive feedback on the negative one using all-pass discrete-time filters which are arranged in a cascade. The piezoelectric actuator as a source of force is used to damp vibration. It is well known that this actuator type has hysteresis which is taken into account when analysing the active vibration control effect. Simulation examples will illustrate theory.

2. Model of the flexible mechanical structure

As assumed the paper deal with the mechanical systems of N degrees of freedom. The response of these mechanical systems to external forces describes the equation of motion in a matrix form

$$\mathbf{M}\ddot{\mathbf{y}} + \mathbf{C}\dot{\mathbf{y}} + \mathbf{K}\mathbf{y} = \mathbf{F} \tag{1}$$

where $\mathbf{M}$, $\mathbf{C}$ and $\mathbf{K}$ denote the mass, damping, and stiffness matrices, respectively, $\mathbf{F}$, $\mathbf{y}$, $\dot{\mathbf{y}}$, and $\ddot{\mathbf{y}}$ are the force, linear displacement, velocity and acceleration vectors, respectively. Note that matrices $\mathbf{M}$, $\mathbf{C}$ and $\mathbf{K}$ are square symmetric of the size $N \times N$. The linear displacement can be considered as a coordinate and refers to a specific node of the mechanical system. An additional term on the left side of the equation of motion that is proportional to the velocity vector indicates the presence of viscous damping as a dissipative force. The damping matrix is assumed to be of the Rayleigh type $\mathbf{C} = \alpha\mathbf{M} + \beta\mathbf{K}$, where α, β are the constants of proportionality. The dependence of the damping ratio ξ on frequency f in hertz can be seen from the formula $\xi = \pi(\alpha/f + \beta f)$. The numerical value of the constants of proportionalit are as follows $\alpha = 0{,}159\ [\mathrm{s}^{-1}]$, $\beta = 0.0000411\ [\mathrm{s}]$.

The possible vibration frequency ω_k of the undamped system is determined by solving the equation $(\mathbf{K} - \omega_k^2\mathbf{M})\mathbf{u}_k = \mathbf{0}$, where a vector $\mathbf{u}_k$ is known in mathematics as an eigenvector. The

number of solutions is equal to N and all eigenvectors can be arranged into a matrix $\mathbf{U}$. Since the eigenvectors can be scaled by arbitrary nonzero factors, we must normalize them to make them unique. The normalized eigenvectors are arranged into the modal matrix $\mathbf{V}=[\mathbf{v}_1,\mathbf{v}_2,...,\mathbf{v}_N]$. Normalization of the matrix of eigenvectors is chosen so that it fulfils the equation $\mathbf{V}^T\mathbf{M}\mathbf{V}=\mathbf{I}$, where $\mathbf{I}$ is the matrix of identity.

The external forces $\mathbf{F}=[F_1,F_2,...,F_N]^T$ are the inputs of the mechanical system and displacement $\mathbf{y}=[y_1,y_2,...,y_N]^T$ are its outputs. The matrix $\mathbf{H}$ which entries $H_{r,q}(\omega)$ relate the force acting at the node indexed by q to the displacement y_r is a transfer matrix. The individual entries of the matrix $\mathbf{H}$ as a function of the angular frequency ω are as follows

$$H_{r,q}(\omega)=\sum_{n=1}^{N}\frac{v_{n,r}v_{n,q}}{\Omega_n^2-\omega^2+j2\xi_n\Omega_n\omega},\quad r,q=1,2,...,N \tag{2}$$

where $v_{n,r}$, $v_{n,q}$, $n,r,q=1,...,N$ are the elements of the N-dimensional normalized eigenvector $\mathbf{v}_n=[v_{n,1},v_{n,2},...,v_{n,N}]^T$ which is associated with the natural frequency Ω_n and relative damping ξ_n. The coordinates $v_{n,1},v_{n,2},...,v_{n,N}$ determine a vibration or mode shape. The transfer function (2) of the system is a sum of the transfer functions of the second order systems which correspond to the vibration mode indexed by n. The product $k_n=v_{n,r}v_{n,q}$ for given value of indexes r and q is called a modal constant and depends on the modal shapes for the natural frequency Ω_n. The modal constant plays a critical role for the type of feedback.

3. Model of the cantilever beam

This paper is focused on active vibration control of the cantilever beams. Coordinates and dimensions are defined in Fig. 1. The beam is divided into N elements. As the motion is assumed only in the direction of y, therefore the degree of freedom is equal to N.

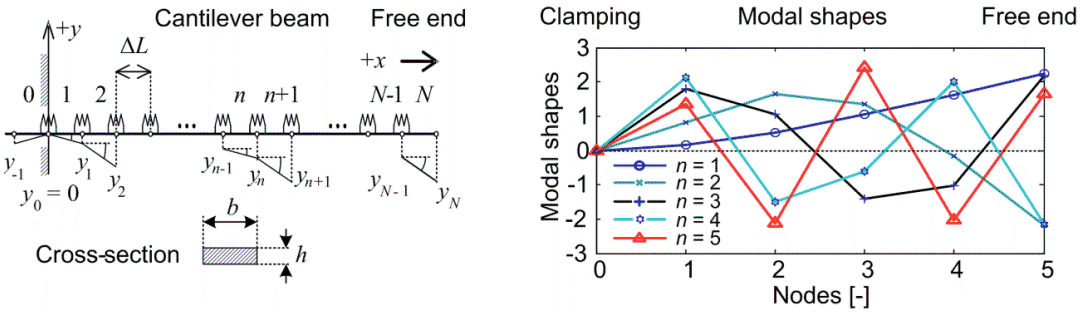

Figure 1: Coordinates and elements of a cantilever beam, modal shapes.

The stiffness and mass matrices for the cantilever beam have been derived in the preceding publications [2, 3, 4, 5]. For calculation of the stiffness matrix, a bending stiffness is needed. This stiffness K_δ relates the applied bending moment M to the resulting rotation $\Delta\delta$ of the elementary beam

$$K_\delta=M/\Delta\delta=EI_z/\Delta L, \tag{3}$$

where $E=2.14\times10^{11}\left[\mathrm{N/m^2}\right]$ is Young's modulus of the beam material, $I_z=bh^3/12$ is the area moment of inertia of the beam cross-section with respect to the axis which is perpendicular to the xy- plane.

The stiffness and mass matrix has the following form

$$\mathbf{K}=\frac{K_\delta}{\Delta L^2}\begin{bmatrix} 7 & -4 & 1 & & & & & & \\ & & \vdots & \vdots & \vdots & \vdots & \vdots & & \\ & & 1 & -4 & 6 & -4 & 1 & & \\ & & \vdots & \vdots & \vdots & \vdots & \vdots & & \\ & & & & & & 1 & -2 & 1 \end{bmatrix},\quad \mathbf{M}=\begin{bmatrix} B & A & & & & & & & \\ & \vdots & \vdots & \vdots & \vdots & & & & \\ & & A & B & A & & & & \\ & & \vdots & \vdots & \vdots & \vdots & & & \\ & & & & & A & B/2 & & \end{bmatrix}, \tag{4}$$

where parameters A and B of the mass matrix are as follows

$$A=\frac{\Delta m}{4}\left\{1-\frac{1}{3}\left[1+\left(\frac{h}{\Delta L}\right)^2\right]\right\},\ B=\frac{\Delta m}{2}\left\{1+\frac{1}{3}\left[1+\left(\frac{h}{\Delta L}\right)^2\right]\right\} \tag{5}$$

For simulation study a beam with the following parameters is used: length L = 0.5 [m], width b = 0.04 [m], and thickness h = 0.005 [m]. The beam is divided into N = 5 elements. All the natural frequencies are shown in Table 1 and corresponding modal shapes on the right side of Fig. 1.

Table 1: Modal frequencies

Mode	1	2	3	4	5
Frequency [Hz]	19.03	114.3	308.3	575.3	842.5

As is apparent from the modal shapes in Fig. 2, the signs of the modal constants are as follows

$$v_{1,5}v_{1,1}>0,\ v_{2,5}v_{2,1}<0,\ v_{3,5}v_{3,1}>0,\ v_{4,5}v_{4,1}<0,\ v_{5,5}v_{5,1}>0$$

For vibration modes with the index equalled to an odd integer, the modal constants are positive while for the even index the modal constant is negative.

The equation of motion (1) is the second order ordinary differential equation. After the introduction of the substitution of $\mathbf{u}_1=\mathbf{y}$, and $\mathbf{u}_2=\dot{\mathbf{y}}$, the second order equation is divided into two differential equations of the first order. An arrangement of the subsystem which models the beam for any number of elements in the Matlab-Simulink is shown in Fig. 2. Entering the simulation is complete to the initial conditions $\mathbf{u}_1(0)=\mathbf{y}(0)$, and $\mathbf{u}_2(0)=\dot{\mathbf{y}}(0)$. The blocks of the *Gain* type contain the product of the matrix and the vector, and therefore the output is a vector as well.

$$\dot{\mathbf{u}}_1=\mathbf{u}_2$$
$$\dot{\mathbf{u}}_2=\mathbf{M}^{-1}\mathbf{F}-\mathbf{M}^{-1}\mathbf{C}\mathbf{u}_2-\mathbf{M}^{-1}\mathbf{K}\mathbf{u}_1$$

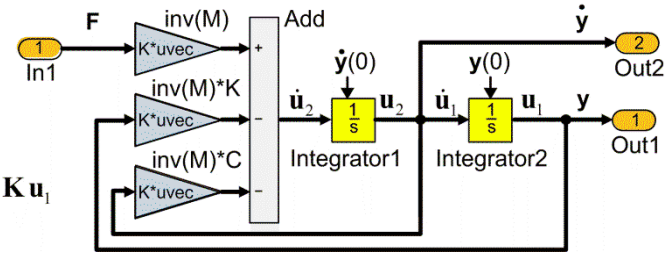

Figure 2: Matlab-Simulink model of the beam.

4. Piezo actuator in the closed-loop

Piezo-actuators generate force or displacement (travel, stroke) which depends on the supply electrical voltage. The relationship between force and displacement describes the working graph which is shown on the left side of Fig. 3. Each curve is determined by the supply voltage. The nominal displacement L_{max} for the maximum supply voltage V_{max} and the blocking force F_{max} are specified in the technical data of the actuator or it can be found by measurements. The blocking force is the maximum force generated by the actuator at the maximum supply voltage and zero travel [7]. Because we use the stacked LVPZT (low voltage PZT type) piezoelectric actuator of the P-844.60 type originated from the PI Company, the catalogue specification of this piezo-actuator is used to plot the working graph in Fig. 3.

The force F which is generated by the piezo-actuator is given by the formula

$$F = F_{\max}\left(V/V_{\max} - L/L_{\max}\right) \tag{6}$$

The travel of the piezo-actuator is equal to the deflection of the beam at the node where the piezo actuator operates with a travel of $L = -y_r$. The piezo-actuator has a finite stiffness, which can be calculated with the use of the blocking force and the nominal displacement.

$$K_P = F_{\max}/L_{\max} = 3000\,[\mathrm{N}]/0.00009\,[\mathrm{m}] = 33\,[\mathrm{MN\ m^{-1}}] \tag{7}$$

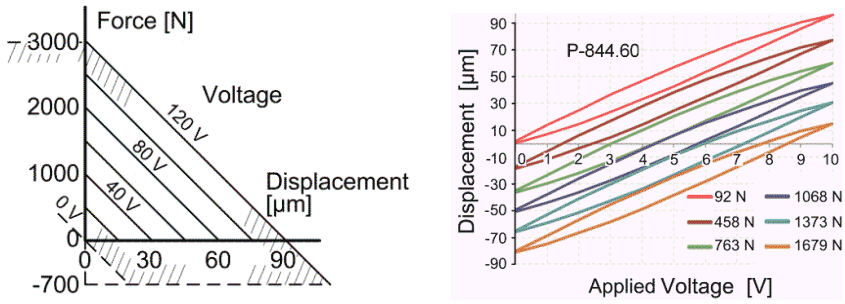

Figure 3: Working graph for the P-844.60 piezo-actuator and hysteresis measurements.

The piezo-actuator exhibits significant hysteresis. The result of the hysteresis measurements is shown on the right side of Fig. 3, which was taken from doctoral theses [6] of J. Los. Dependence of the piezo-actuator displacement on the input electrical voltage was determined for a set of the constant load force. There are several ways how to create a model of hysteresis. For example, a model according to Prandtl-Ishlinskii is based on a backlash in a mechanism. The *Backlash* block of Matlab-Simulink implements a system in which a change in input causes an equal change in output. However, when the input changes direction, an initial change in input has no effect on the output which remains at the previous value. The principle of the piecewise approximation of the output displacement on the input control voltage is shown on the left side of Fig. 4. This diagram also explains the meaning of the parameters that are constant inputs for the other blocks of Matlab-Simulink while the diagram on the right side of this figure shows the result of simulation with the use of 11 *Backlash* blocks. The detailed procedure for calculating the parameters h and w is described in the mentioned dissertation thesis [6].

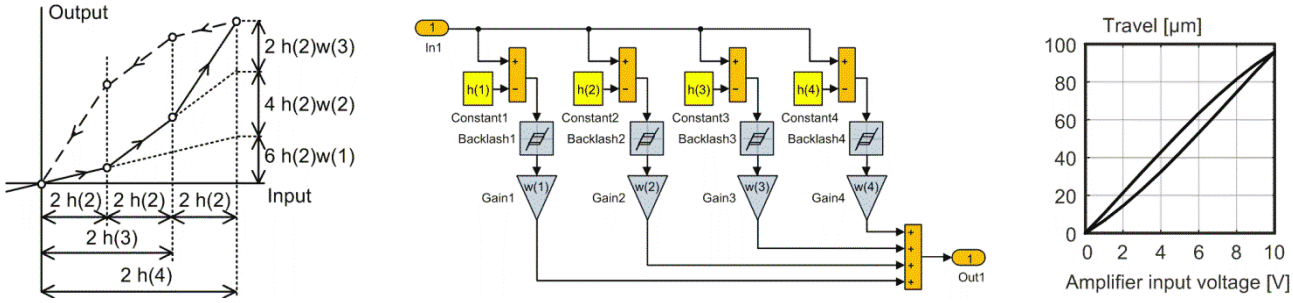

Figure 4: Prandtl-Ishlinskii model of hysteresis.

Just as there are two ways of modelling electric power sources according to the Thévenin theorem and the dual Norton theorem also piezo-actuators can be modelled similarly, i.e. either as a source of force F^* or as a source of displacement y^* with the connection of the inner spring which simulates the piezo-actuator stiffness K_P and is calculated according to (7). Both the solutions are shown in Fig. 5 [7]. In these diagrams, the force is equivalent to the electric current and displacement to the electric voltage. Taking into account the piezo-actuator stiffness, the force acting on the beam must be corrected in both cases as is shown in Fig. 5.

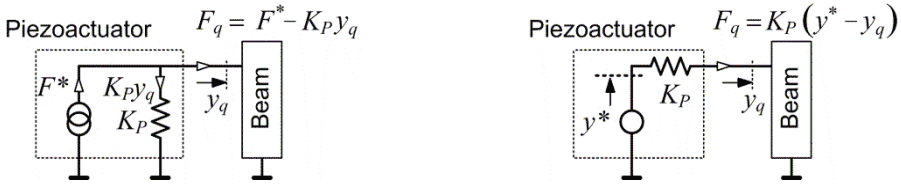

Figure 5: Two ways of connection of piezo actuator and beam models.

Connecting the piezo-actuator to the beam changes the natural frequencies of the complete system in the same way. The effect of the piezo-actuator stiffness on the stiffness matrix for the left equivalent in Fig. 5 can be determined by the same procedure as was created the equation of motion of the beam with the use of the Lagrange's equations. The displacement of the piezo-actuator spring determines the potential energy and after the partial derivative with respect to the coordinate of the node q, the effect on the matrix **K** is found. The stiffness of the piezo-actuator is added to the main diagonal elements of the stiffness matrix **K** which is indexed by q. The actual resonant frequencies for the case where the piezo- actuator is connected to the beam are calculated in Table II. An example of the Frequency Response Function (FRF) $j\omega H_{5,1}(\omega)$ for the input of the force acting at node #1 and the output which is a velocity (change rate of y_5) at the node #5 is shown on the left side of in Fig. 6. The velocity $\dot{y}_5$ is used as it will be described a velocity feedback in the next section.

Table 2: Modal frequencies of the complex system

Mode	1	2	3	4	5
Frequency [Hz]	24.1	155.3	437.8	790.1	2976.7

The magnitude of FRF shows the resonant frequency peaks corresponding to the vibration modes. The resonant amplification for the first and second mode is achieved hundredfold greater compared to the gain in the background of FRF. The modal constants for these natural frequencies have approximately the same absolute value but the opposite sign. The feedback affects contradictory on the stability. It is important that the resonant peaks are well separated, i.e. between them is gap of the amplification of oscillations and the second frequency is nearly a hundred times greater.

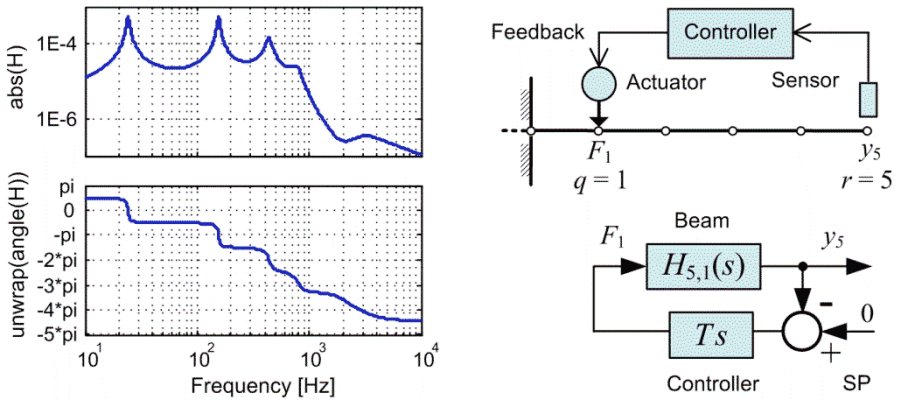

Figure 6: Frequency response function $j\omega H_{5,1}(\omega)$ and AVC system of the cantilever beam.

5. Active vibration control

The purpose of the system for the active vibration control (AVC) is to compensate the effect of a disturbing external force on the vibration of the mechanical structure. The dampening effect of AVC can be assessed by changes in displacement, velocity or acceleration of the selected node of the structure. It can be the free end of the cantilever beam which models a cutting tool or boring bar of the lathe for instance. The result of the active dumping is the minimum motion around the steady-state position and the minimum velocity or acceleration of vibrations.

There are two possible solutions, the collocated and non-collocated active vibration control. For the collocated system, the correcting force acts and the response is measured at the same node. For the non-collocated system, it is assumed that the correcting force acts at the node indexed by q and the vibrations are sensed at the node indexed by $r \neq q$. An example of the non-collocated system is shown on the right side of Fig. 6. The vibration of the free end element of this cantilever beam is sensed at the node $r = 5$ and the correcting force acts at the element just next to the clamped end, therefore $q = 1$.

Mechanical structures are weakly damped. Theoretical analysis shows that for undamped systems there are absent terms of the odd powers of the complex variables s in the Laplace transfer function. The undamped system is at the margin of stability. It has been shown that the most appropriate controller for such systems uses a proportional feedback based on the velocity change of the controlled displacement as it is shown on the right side of Fig. 6. The controller is a derivative type in terms of displacement as a controlled variable. The setpoint (SP) for such closed-loop system is equal to zero. The gain of the velocity feedback is designated by T. The stability of the feedback system determines the position of the pole of the closed-loop transfer function. The beam is a stable system without control due to the natural damping; it does not start to vibrate by itself. The increase of the feedback gain causes one of the poles that are associated with the two lowest resonant frequencies moves away from the instability margin while the other pole is approaching or exceeding the stability margin. For the given beam, which is divided into five elements, and the assumption of the Rayleigh's damping, the locus of the closed-loop poles are shown in Fig. 7. The root locus demonstrates the effect of the controller time constant T change on the system stability. The time constant varies from 0 to 1E6. The poles are calculated as the roots of the polynomial $1 + TsH_{5,1}(s)$.

Because the degree of polynomial equals to ten in the complex variable s, the number of roots, i.e. the number of poles is ten as well. Five pairs of poles are complex conjugate. The stability margin crosses the pole for the mode $n = 2$ and the pole for the mode $n = 4$ approaches this margin.

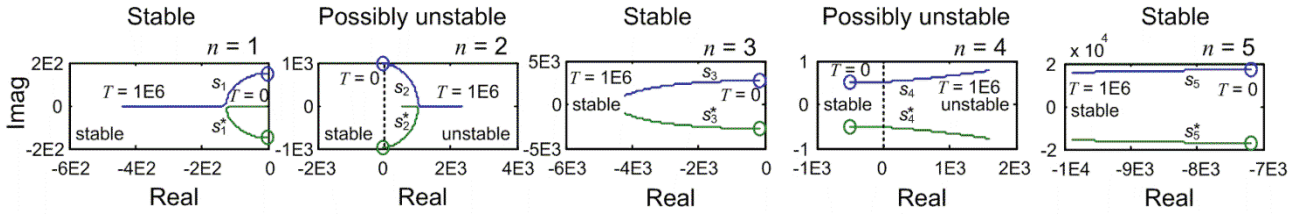

Figure 7: Root locus to demonstrate the effect of the time constant T change.

The analysis shows that the opposite sign of the modal constants reduces the damping effect of velocity feedback. There are two possible ways how to improve the efficiency of the active vibration control of weakly damped systems

- either control each vibration mode separately
- or change the positive feedback to the negative one.

Both the methods indicate the transition of the controller design from the frequency range from zero to infinity to the control in a narrow frequency band.

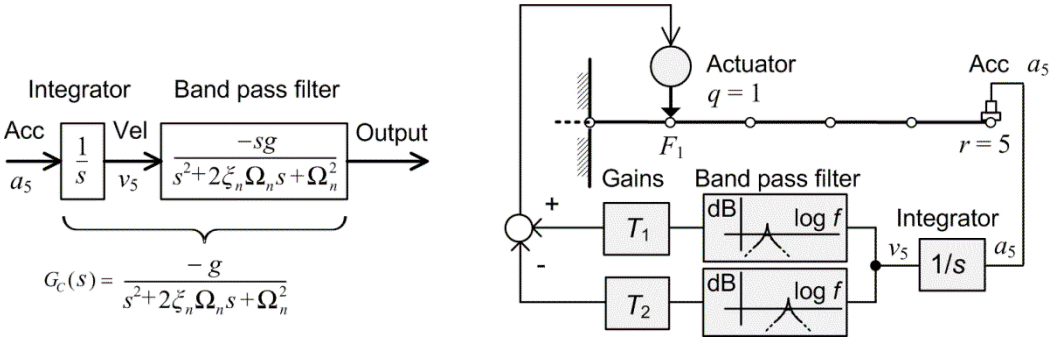

Figure 8: Principle of Positive Position Feedback (PPF).

The first possible solution with the filter of the band-pass type is shown in Fig. 8. This arrangement of the AVC system is called a Positive Position Feedback (PPF) controller [1]. In the mentioned figure, PPF is intended for two resonant frequencies with the negative and positive feedbacks. The input signal of the filter is a signal of the velocity type because a controller of the proportionality type is used. The velocity signal is obtained by integrating the acceleration signal with respect to time. The acceleration is measured on the free end of the beam as the controlled variable. The integration and band-pass filtering together form a low-pass filter, whose transfer function has been designed previously by many authors [1]. The filter is of the second order and therefore causes the least possible delay in the control loop. The output of this filter is amplified as necessary. The frequency range of the controller is restricted to a narrow band around the resonant frequency.

The second method for controlling the weakly damped systems is converting the positive feedback to negative with the use of an all-pass filter. This type of the frequency filter modifies the phase of the harmonic signal at the output compared to the input without changing the amplitude of the signal frequency components. The filter of this type of the first-order type changes the phase from 0 to π radians in the frequency range from 0 to infinity. The all-pass filter of the second order shown on the left and middle of Fig. 9 doubles the phase change. For the possibly unstable modes, it is necessary to change the phase by π at the resonant frequency of this vibration mode whose modal constant is to be changed from the negative to positive value. The advantage of this filter is the controllable rate of the change of phase with respect to change of the frequency by setting the value of the relative damping parameter ξ_{APF} .

$$G_{APF,n}(s) = \frac{s^2 - 2\xi_{APF}\,\omega_n\, s + \omega_n^2}{s^2 + 2\xi_{APF}\,\omega_n\, s + \omega_n^2}$$

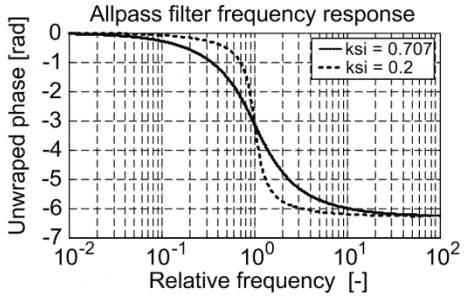

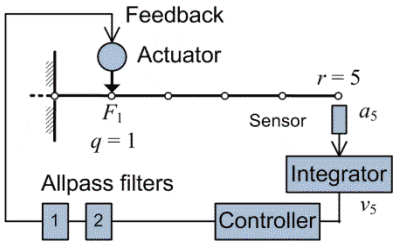

Figure 9: All-pass filter frequency response (ksi = ξ_{APF}).

Since $\left|G_{APF,n}(j\omega)\right| = 1$ only a phase frequency response for two values of the damping parameter ξ_{APF} is shown in the middle of Fig. 9. The all-pass filters are connected in series (cascade) with the controller as it is shown on the right of Fig. 9. The count of these filters is as many as the count of the negative modal constants.

6. Simulation results

The effect of the all-pass filter on the damping of the beam vibration demonstrates the control system responses with the use of the two all-pass filters in the closed loop and without them as is shown on the right of Fig. 9. One of the all-pass filters is tuned to the frequency of the second vibration mode, and the second one to the frequency of the fourth vibration mode. The beam is excited by a short pulse after 1 second from the beginning of the simulation. During the interval of 1 second, the piezo actuator is gradually prestressed by the force of 1500 N. The decaying vibration response without any active vibration control (AVC OFF) is shown on the left of Fig. 10. The effect of ACV without using the all-pass filter (ALL-PASS FILTER OFF) is shown in Fig. 6. Due to the stability, the open-loop gain can be set less or equal to 4. The serial connection of two all-pass filters in the cascade allows increasing the gain of the open-loop in such a way that the time constant T may be increased up to the value of 25 but less than 30 with correspondingly increasing the damping effect as is shown on the right of Fig. 10. The result of the experiment for the acceleration of the beam free end is shown in Fig. 11. The beam has the same dimensions as in the simulation study.

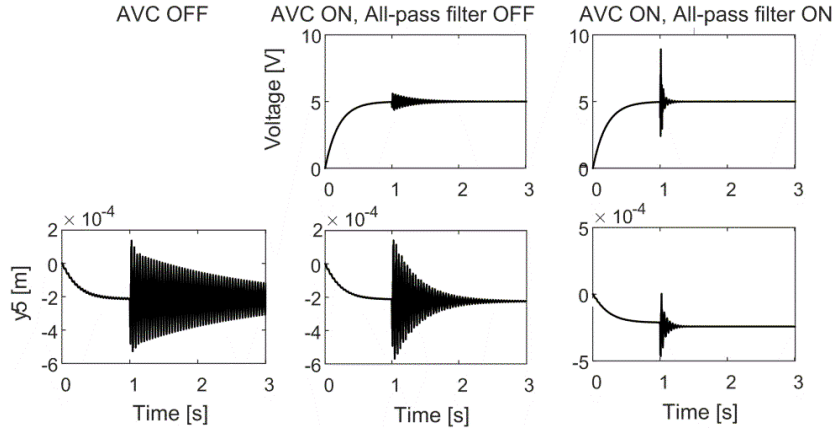

Figure 10: Decaying vibration without any active control and two ways of the active vibration controls.

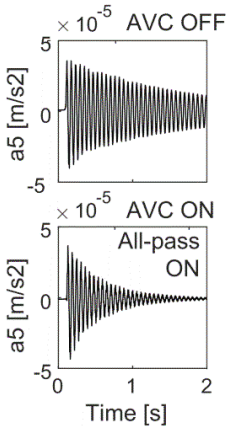

Figure 11: Experiment.

7. Conclusion

The Matlab-Simulink model of the cantilever beam was designed using the method based on the modal analysis. Because piezo-actuators have considerable hysteresis, the beam model is extended by a hysteresis model based on a backlash in a mechanism. Mechanical systems are weakly damped. Stable active damping cannot be designed by classical methods. Some modes for these systems become potentially unstable. The paper describes the method that converts the positive feedback to the negative feedback using the all-pass filter. The effect of the all-pass filter on increasing the damping by shortening the impulse response has been verified by simulation approach.

ACKNOWLEDGMENT

This research has been done in the framework of the project No: SP2017/106 „Advanced Methods for Machine and Process Control“ supported by the Ministry of Education, Youth and Sports.

REFERENCES

1 Preumont, A., Active Vibration Control of Active Structures. Kluwer Academic Publishers, 1997.

2 P. Šuránek, M. Mahdal, J. Tůma and J. Zavadil, “Modal analysis of the cantilever beam”. Proceedings of the 14th International Carpathian Control Conference (ICCC 2013), May 26 - 29 2013, Rytro, Poland, pp. 367-372. ISBN: 978-1-4673-4490-6.

3 P. Šuránek, M. Mahdal, J. Tůma, “Modelling and Simulation of an Active Damped Structure”, In: 15th International Carpathian Control Conference (ICCC 2014), 28-30 May 2014, Velké Karlovice, Czech Republic, IEEE Catalog Number: CFP1442L-CDR ISBN: 978-1-4799-3527-7.

4 J. Tůma, P. Šuránek, M. Mahdal, “Vibration damping of the cantilever beam with the use of the parametric excitation”, In: Proceedings of the 21st International Congress on Sound and Vibration (ICSV 21), 13-17 July 2014, Beijing, China. Paper 905.

5 J. Tůma, P. Šuránek, M. Mahdal, R. Wagnerová, “Linear piezoactuators in systems of the active vibration control”, In: Proceedings of the 23rd International Congress on Sound and Vibration (ICSV 23), 10-14 July 2016, Athens Greece.

6 J. Los, “Mechatronické systémy s piezoaktuátory”, Doctoral thesis, VSB – Technical University of Ostrava, 2016.

7 S. O. Reza, Moheimani, A. J. Fleming, Piezoelectric Transducers for Vibration Control and Damping. Springer, ISBN-13:9781846283314.